DOI https://doi.org/10.59887/2073-6673.2025.19(1)-2

EDN https://elibrary.ru/jtkefu

УДК 550.361+550.362

© *A. Ya. Golmshtok*[1]*, *A. L. Piskarev*[2,3], 2026

© Translated from Russian: *E.S. Kochetkova*, 2026

[1]Shirshov Institute of Oceanology, Russian Academy of Sciences, 36 Nakhimovsky Prosp., Moscow, 117997, Russia
[2]Gramberg All-Russia Research Institute of Geology and Mineral Resources of the World Ocean (VNIIOkeangeologia), 124 lit. A Moika River Emb., St. Petersburg, 190121, Russia
[3]St Petersburg State University, 7–9 Universitetskaya Emb., St Petersburg, 199134, Russia
*golmshtok@gmail.com

The remarks on the mid-ocean ridges topography formed synchronously with sedimentation on their surface (using the Nansen and Amundsen Basins, Arctic Ocean, as an example)

Received 26.10.2025, Revised 08.01.2026, Accepted 16.01.2026

Abstract

A solution to the problem of the thermal regime of the forming oceanic lithosphere during sedimentation on its surface is presented. This allows us to assess the causes of the significant contrast in sea depths in the Nansen and Amundsen Basins, located in the Arctic Ocean on either side of the Gakkel Ridge. This paper examines the role of both the gravitational load and the thermal insulation effect of the accumulating sedimentary cover on the formation of the relief of the basins surrounding the ridge. It is shown that neglect for the thermal effect of sedimentation on sea depth in the basins in isostatic models leads to errors of several hundred meters. Estimated sea depths in the Nansen and Amundsen Basins, calculated for lithosphere of different ages, taking into account both the gravitational and thermal effects of sedimentation, are comparable to actual depths. The calculated differences in sea depth at reference points in the central regions of both basins are also close to the actual depths.

Keywords: ocean, ridge, Nansen Basin, Amundsen Basin, sedimentation, lithosphere, temperature, phase transition

© *А. Я. Гольмшток*[1]*, *А. Л. Пискарев*[2,3], 2026

© Перевод с русского: *Е. С. Кочеткова*, 2026

[1]Институт океанологии им. П.П. Ширшова РАН, 117997, Москва, Нахимовский проспект, д. 36
[2]Всероссийский научно-исследовательский институт геологии и минеральных ресурсов Мирового Океана им. акад. И.С. Грамберга (ВНИИОкеангеология), 190121, Санкт-Петербург, Английский пр-т, д. 1
[3]Санкт-Петербургский государственный университет — Институт наук о Земле, 199134, Санкт-Петербург, Университетская наб., д. 7–9
*golmshtok@gmail.com

Замечания о топографии срединно-океанических хребтов, сформированных синхронно с осадконакоплением на их поверхности (на примере котловин Нансена и Амундсена, Северный Ледовитый океан)

Статья поступила в редакцию 26.10.2025, после доработки 08.01.2026, принята в печать 16.01.2026

Аннотация

В статье приводится решение задачи о тепловом режиме образующейся океанической литосферы при осадконакоплении на ее поверхности, позволяющее оценить причины существенного контраста глубин моря в котловинах Нансена и Амундсена, окаймляющих хребет Гаккеля в Северном Ледовитом океане. Поскольку действие накапливающегося осадочного покрова на океаническую литосферу складывается как из его гравитационной нагрузки, так и его теплоизолирующего эффекта, в работе выполнено исследование их роли на формирование рельефа окружа-

Ссылка для цитирования: *Гольмшток А.Я.*, *Пискарев А.Л.* Замечания о топографии срединно-океанических хребтов, сформированных синхронно с осадконакоплением на их поверхности (на примере котловин Нансена и Амундсена, Северный Ледовитый океан) // Фундаментальная и прикладная гидрофизика. 2026. Т. 19, № 1. С. 32–44. EDN JTKEFU. https://doi.org/10.59887/2073-6673.2025.19(1)-2

For citation: Golmshtok A. Ya., Piskarev A.L. The remarks on the mid-ocean ridges topography formed synchronously with sedimentation on their surface (using the Nansen and Amundsen Basins, Arctic Ocean, as an example). *Fundamental and Applied Hydrophysics*. 2026;19(1):32–44. https://doi.org/10.59887/2073-6673.2025.19(1)-2

ющих хребет котловин. Показано, что неучет в изостатических схемах роли теплового воздействия осадконакопления на глубину моря в котловинах может привести к ошибкам порядка нескольких сотен метров. Оценочные глубины моря в котловинах Нансена и Амундсена, вычисленные для литосферы различного возраста с учетом как гравитационного, так и теплового влияния осадконакопления, вполне удовлетворительно сопоставимы с реально существующими. Расчетные перепады глубин моря в опорных точках в центральных областях обеих котловинах весьма близки к реальным. Выполненное моделирование образования океанической литосферы в центральной области Евразийского бассейна Северного Ледовитого океана с учетом как гравитационного, так и теплового влияния процесса осадконакопления показывает, что наблюдаемое в этой области различие глубин в котловинвх Нансена и Амундсена действительно определяется мощностями их осадочных покровов и является вполне закономерным.

Ключевые слова: океан, хребет, котловина Нансена, котловина Амундсена, осадконакопление, литосфера, температура, фазовый переход

1. Introduction

In the «open ocean» (i. e., without sediments), basins located on either side of spreading mid-ocean ridges are, as a rule, arranged nearly symmetrically with respect to the ridge axis. A markedly different configuration is observed in the structure of the basins flanking the Gakkel Ridge, which forms part of the Mid-Atlantic Ridge system.

The sea depth in the Nansen Basin (NB) is significantly shallower than in the Amundsen Basin (AB). This difference, reaching 1 km or more, has been noted by virtually all researchers working in the Eurasian Basin of the Arctic Ocean [1]. The principal explanation typically invoked is that sediment thickness in the Nansen Basin exceeds that in the Amundsen Basin by more than a factor of two. Accordingly, the sedimentary load imposed on the oceanic lithosphere, and thus its subsidence, should differ between the two basins. Nevertheless, it remains unclear why the resulting depth contrast is so large.

When accounting for the load of a sedimentary cover accumulating on the oceanic lithosphere simultaneously with its formation at the spreading axis, the conventional isostatic scheme is usually applied to these basins. In this approach, at a given location with a known lithospheric age, the lithospheric thickness is taken to be equal to that of a lithosphere of the same age in the «open ocean» (i. e., without sediments) [1]. In such a model, sedimentation exerts only a gravitational effect on an already formed lithosphere, promoting its subsidence together with the sediments and thereby modifying sea depth.

However, this approach does not consider the influence of the accumulating sedimentary cover on the thermal regime of the oceanic lithosphere itself. This influence leads to slower cooling and, consequently, to a reduction in lithospheric thickness compared to the open-ocean case. The magnitude of this effect may be substantial, because the density of lithospheric material is considerably higher than that of sediments.

Below, we present estimates of the combined gravitational and thermal effects of sedimentation occurring synchronously with the formation of oceanic lithosphere on the evolution of sea depth in the Nansen and Amundsen basins adjacent to the Gakkel Ridge.

2. Thermal regime of the forming oceanic lithosphere overlain by accumulating sediments

In the zone of mid-ocean ridges, lithospheric plates are continuously formed. Under the action of extensional forces (primarily slab pull at subduction zones and related mechanisms), two plates located on either side of the ridge diverge. As a result, hot mantle material (basaltic melt) rises from below and fills the developing gap, forming along the ridge a narrow and elongated vertical dike-like body whose upper surface comes into contact with seawater and acquires its temperature. Because spreading proceeds discretely, with short intervals between magmatic intrusions, the injected melt cools and solidifies between spreading pulses, forming a thin “neck” in the vertical cross section. When the continuing extensional stresses exceed the strength of this neck, rupture occurs and a new opening forms in the lithosphere, again filled by basaltic melt.

As the plates move away from the ridge axis, not only the basaltic material within magma chambers cools and crystallizes, but also the partially molten basaltic material in the asthenosphere. With time, cooling penetrates progressively deeper portions of the asthenosphere, resulting in a gradual increase in oceanic lithospheric thickness. On geological time scales, the discrete character of spreading may be neglected, and the spreading rate may be treated as constant. Lithospheric thickness then increases continuously with distance from the ridge axis — the constructive plate boundary. The colder oceanic lithosphere possesses negative buoyancy relative to the hot asthenosphere and therefore tends to subside into it. This subsidence increases with lithospheric thickness and, consequently, with age. As a result, basins flanking the ridge are formed in an approximately symmetrical manner on both sides of the spreading center.

The temperature beneath the plate (including along the full depth beneath the ridge axis) is equal to the temperature of the upper mantle. As noted above, the upper surface of the plate acquires the temperature of bottom water. Thus, the surface of the newly intruded, laterally extensive mantle-derived dike — initially at upper-mantle temperature — undergoes an abrupt temperature change to bottom-water temperature. During lateral displacement away from the ridge, the interior of the dike cools. When new melt intrudes, the adjacent rocks formed during the previous intrusion have not yet cooled sufficiently for lateral heat flow from the newly formed dike to become comparable to vertical heat flow. Heat flow along the strike of the dike is negligible, because intrusion occurs simultaneously along its entire length, ensuring identical thermal conditions along strike and preventing longitudinal heat transfer. If horizontal conductive heat transfer across the dike is neglected relative to vertical heat transfer, that is, if the dike is treated as thermally insulated laterally, then cooling of this narrow vertical body occurs only in the vertical direction. This process is mathematically equivalent to the cooling of a thin, laterally insulated vertical rod subjected to an abrupt change in temperature at its upper end. The cooling of such a rod is described by the same mathematical formulation as cooling of a homogeneous half-space under an instantaneous change in boundary temperature. In other words, neglecting horizontal molecular heat transfer, heat flux in the retreating dike proceeds vertically, as in the classical half-space cooling model of oceanic lithosphere formation [2].

If sedimentation occurs simultaneously with the formation of oceanic lithosphere, the thermal regime of the lithosphere is altered. In the general case, its description requires numerical methods. However, since the purpose of the present study is to estimate the possible causes of the pronounced depth difference between the Nansen and Amundsen basins, we restrict ourselves to the following simplified consideration.

2.1. Thermal conditions in the medium

For simplicity, we assume that the thermophysical properties of the sediments do not vary with depth, and that both the mineral framework and pore water are incompressible.

The formation of a sedimentary layer itself modifies the thermal regime of the underlying substrate. This occurs, first, because deep heat is expended to warm newly deposited cold sediments after their accumulation on the seafloor and, second, because of the insulating effect of the sedimentary cover, whose thermal conductivity is significantly lower than that of the crystalline lithosphere. Heat consumption increases with time and depends strongly on the thickness of the sedimentary cover $h(t)$. The insulating effect impedes heat loss from the lithosphere, resulting in anomalous heating of the lower part of the sedimentary layer and the upper part of the crystalline lithosphere compared with the case where no contrast in thermophysical properties exists between sediments and lithosphere.

Let the sedimentary cover (medium 0) be characterized by thermal conductivity λ_0, thermal diffusivity a_0 and density of the sediment mineral skeleton ρ_{sk}. The parameters of the lithosphere (medium 1) and asthenosphere (medium 2) will be denoted λ_2, a_1 and λ_2, a_2 respectively.

We place the origin of coordinates at the lithosphere surface (i. e., at the base of the sedimentary cover) and direct the axis z upward. In this coordinate system, the lithosphere and asthenosphere occupy the region $z \le 0$.

2.1.1. Model of sedimentary cover formation on synchronously forming oceanic lithosphere

The porosity of the sedimentary material at level z is determined by lithostatic pressure caused by the weight of overlying sediments. In other words, porosity φ at depth z is a function of $\tilde{z} = h(t) - z$ and may be written as $\varphi(\tilde{z}) = \varphi(h(t) - z)$.

If the time-varying sedimentation rate $u_s(t)$ is known, then, taking into account that in a sedimentary column $0 \le z \le h(t)$ the mass of mineral framework material accumulated over time t and subjected to compaction (porosity $\varphi(\tilde{z})$) must be equal to the mass of the same substance that would accumulate in an uncompacted column $0 \le z \le h_0 = \int_0^t u_s(\tau)d\tau$ over the same time interval (porosity φ_0), we obtain an equation for determining sediment thickness $h(t)$ at any time since the onset of oceanic lithosphere formation:

$$h(t) = \int_0^{h(t)} \varphi(\tilde{z})d\tilde{z} + (1-\varphi_0)\int_0^t u_s(\tau)d\tau. \tag{1}$$

Here φ_0 is the porosity at the surface of the accumulating sediments.

In addition to sediment compaction, when describing formation of a sedimentary cover on oceanic lithosphere formed after complete continental rupture, one must consider that the initial phase of spreading is often characterized by proximity of sediment sources (typically river deltas) to the spreading axis. This results in a high initial sedimentation rate. As spreading proceeds, the axis moves farther from the sediment source, and the sediment flux to the axis decreases. The combined effects of sediment compaction and increasing distance between the spreading axis and sediment source lead to a situation in which, for a homogeneous accumulating layer, sediment thickness as a function of time is always represented graphically by a monotonically increasing, progressively flattening curve. This curve resembles a function proportional to the square root of time since the onset of sedimentation, which is equivalent to the age of the oceanic lithosphere.

This statement is illustrated in Fig. 1, which shows solutions of equation (1) (solid lines) together with the approximating dependencies described above (dashed lines):

$$h_s(t) = \alpha_s\sqrt{t}. \tag{2}$$

For example, the sedimentation rate $u_s(t)$ was chosen here as a dependence

$$u_s(t) = a\exp(-bt) + c, \tag{3}$$

and porosity $\varphi(\tilde{z})$ (where $\tilde{z}$ is depth measured from the sediment surface) is described by Athy's law [4]:

$$\varphi(\tilde{z}) = \varphi_0 \exp(-k_s\tilde{z}). \tag{4}$$

Here: k_s is the compaction coefficient (for terrigenous sediments, typical values k_s are 0.4–0.5 km^{-1}, if depth is measured in kilometers).

Taking into account the above, since the clarification of the reason for the strong difference between the sea depths in the Nansen and Amundsen basins is, as stated above, of an evaluative nature, we will restrict ourselves to case (2), briefly considered in work [4].

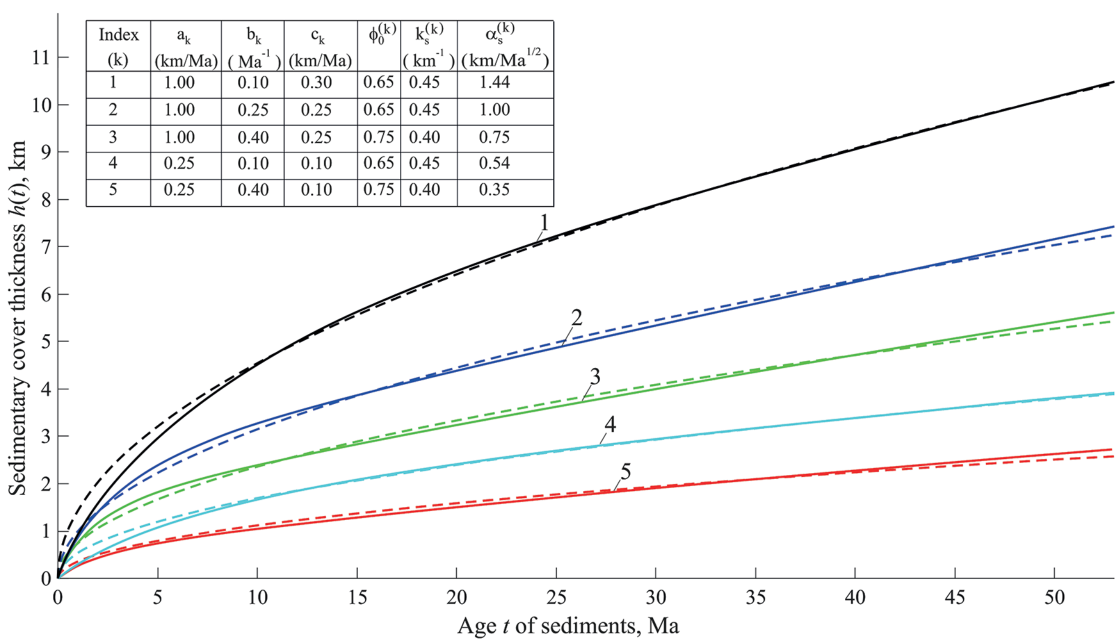

Index (k)	a_k (km/Ma)	b_k (Ma^{-1})	c_k (km/Ma)	$\varphi_0^{(k)}$	$k_s^{(k)}$ (km^{-1})	$\alpha_s^{(k)}$ (km/Ma$^{1/2}$)
1	1.00	0.10	0.30	0.65	0.45	1.44
2	1.00	0.25	0.25	0.65	0.45	1.00
3	1.00	0.40	0.25	0.75	0.40	0.75
4	0.25	0.10	0.10	0.65	0.45	0.54
5	0.25	0.40	0.10	0.75	0.40	0.35

Fig. 1. Example of the dependence of sediment thickness $h(t)$ on age. The solid line is the solution to equation (1); the dashed line is the approximating dependence (2); α_s is the coefficient in this approximating dependence; a_k, b_k, c_k are the coefficients in dependence (3); φ_0, k_s are the parameters in Athy's law (4). Ma — million years ago

2.1.2 Derivation of the Main Relations

At the phase boundary between the lithosphere and the asthenosphere (surface $z = \xi(t)$) a constant phase transition temperature T_{ph} is maintained. This temperature is taken to be equal to the solidus temperature of the most fusible lithospheric rocks (basalts). At this boundary the Stephan's condition for the conductive heat flow $q_j(z, t) = -\lambda_j \partial T_j(z, t)/\partial z (j = 1,2)$ is also satisfied:

$$q_1\big|_{z=\xi} - q_2\big|_{z=\xi} = -L\Delta\rho \frac{d\xi(t)}{dt}, \tag{5}$$

where $\Delta\rho$ is the volumetric density of melt (in asthenospheric material) that undergoes solidification, and L is the latent heat of crystallization (enthalpy), equal to the amount of thermal energy released upon solidification of a unit mass of melt.

Without loss of generality, we assume that the temperature at the sediment surface is maintained equal to the constant bottom water temperature T_s and that the vertical heat flow in the lithosphere is much greater than the lateral heat flow. Thus, in the considered medium, the sediment layer (layer 0) occupies the region $0 \le z \le h_s(t)$. Layer number 1 is the oceanic lithosphere, whose thickness varies with time and equals $H_L(t) = |\xi(t)|$. The lithosphere is underlain by the asthenosphere (layer number 2), occupying the half-space $z \le \xi(t)$.

The temperature in each layer with number j satisfies the heat conduction equation

$$a_j \frac{\partial^2 T_j(z,t)}{\partial z^2} - \frac{\partial T_j(z,t)}{\partial t} = 0, \tag{6}$$

the boundary conditions:

$$\begin{gathered} T_0\left(z = \alpha_s \sqrt{t}, t\right) = T_s; \qquad T_0(z=0,t) = T_1(z=0,t); \\ \lambda_0 \frac{\partial T_0(z,t)}{\partial z}\bigg|_{z=0} = \lambda_1 \frac{\partial T_1(z,t)}{\partial z}\bigg|_{z=0}; \qquad T_1(z,t)\big|_{z=\xi(t)} = T_2(z,t)\big|_{z=\xi(t)} = T_{ph}; \end{gathered} \tag{7}$$

and the initial condition:

$$T_2(z, t=0) = T_m. \tag{8}$$

At the initial moment, the asthenosphere is assumed to be isothermal at a suprasolidus temperature, i. e., $T_m > T_{ph}$.

All three layers of the medium (sedimentary cover, lithosphere, and asthenosphere) have moving boundaries: the surface of the sedimentary cover and the lithosphere–asthenosphere phase boundary.

Using the similarity principle for the heat conduction equation and solving the entire system (6) together under conditions (7), (8), we obtain expressions for the thickness of the oceanic lithosphere beneath the sedimentary layer:

$$H_L(t) = \beta\sqrt{t}, \qquad \beta \ne \mathrm{f}(t) \tag{9}$$

and for the temperature in each layer:

$$T_0(z,t) = T_s + \left(T_{ph} - T_s\right) \frac{\mathrm{erf}(v) - \mathrm{erf}\left(\dfrac{z}{2\sqrt{a_0 t}}\right)}{\mathrm{erf}(v) + \gamma\,\mathrm{erf}(u)}, \quad z \ge 0, \tag{10}$$

$$T_1(z,t) = T_{ph} - \gamma\left(T_{ph} - T_s\right) \frac{\mathrm{erf}(u) + \mathrm{erf}\left(\dfrac{z}{2\sqrt{a_1 t}}\right)}{\mathrm{erf}(v) + \gamma\,\mathrm{erf}(u)}, \quad -\beta\sqrt{t} \le z \le 0, \tag{11}$$

$$T_2(z,t) = T_m - \left(T_m - T_{ph}\right) \frac{\mathrm{erfc}\left(\dfrac{|z|}{2\sqrt{a_2 t}}\right)}{\mathrm{erfc}(\sqrt{a_1/a_2}\,u)}, \quad z \le -\beta\sqrt{t}, \tag{12}$$

where

$$v = \frac{\alpha_s}{2\sqrt{a_0}}, \qquad \gamma = \frac{\lambda_0}{\lambda_1}\sqrt{\frac{a_1}{a_0}}, \qquad u = \frac{\beta}{2\sqrt{a_1}}, \tag{13}$$

$\mathrm{erf}(x)=\frac{2}{\sqrt{\pi}}\int_0^x \exp(-s^2)ds$ is the Gaussian error function, and $\mathrm{erfc}(x)=\frac{2}{\sqrt{\pi}}\int_x^\infty \exp(-s^2)ds$ — is the complementary error function.

Using equation (5) together with relations (10)–(13), we obtain an equation for β or u

$$\gamma\frac{\left(1-T_s/T_{ph}\right)\exp(-u^2)}{\mathrm{erf}(v)+\gamma\,\mathrm{erf}(u)}-\gamma_1\frac{\left(T_m/T_{ph}-1\right)\exp(-a_1/a_2u^2)}{\mathrm{erfc}(\sqrt{a_1/a_2}\,u)}=\mu u, \tag{14}$$

where

$$\gamma_1=\frac{\lambda_2}{\lambda_1}\sqrt{\frac{a_1}{a_2}},\qquad \mu=\sqrt{\pi}\frac{L\Delta\rho a_1}{\lambda_1 T_{ph}}. \tag{15}$$

For our problem, we adopt the following parameter values: T_m = 1350 °C = 1623.15 K is the asthenosphere temperature, equal to the basalt liquidus temperature; T_m = 1350 °C; T_{ph} = 1100 °C = 1373.15 K; T_s = 3 °C = = 276.15 K; L = 400 kJ/kg; λ_1 = 3 W/(m · K), λ_2 = 4 W/(m · K); $a_1 = a_2 = 7\cdot 10^{-7}$ m²/c, $\rho_L^0 = 3330$ kg/m³; $\alpha_L = 3.3\cdot 10^{-5}$ K^{-1} — the coefficient of volumetric thermal expansion of lithospheric (asthenospheric) material; $\Delta\rho = \rho_b\delta_m$, where ρ_b = 2900 kg/m³ is the density of basalt, δ_m = 0.05 is the volume fraction of crystallizing basaltic melt; ρ_w = 1032 kg/m³ is the density of seawater at salinity 35 ‰.

The sediment thermal conductivity λ_s at a point z is found from the effective medium model [5] where λ_{sk} = 2.5 W/(m · K) is the thermal conductivity of the mineral skeleton of the sediment, λ_w = 2.5 W/(m · K) is the thermal conductivity of pore water.

The thermal diffusivity a_s of the sedimentary material at point z is defined as

$$a_s=\frac{\lambda_s}{\widetilde{\rho C}_s}=\frac{\lambda_s}{(1-\varphi)\rho_{sk}C_{sk}+\varphi\rho_w C_w}, \tag{16}$$

where ρ_{sk}, C_{sk} are the density and heat capacity of the solid framework material, and ρ_w, C_w are the corresponding quantities for water.

Since our model assumes that the thermophysical properties of sediments do not change with depth beneath the bottom, we will use their z-average values for each layer with thickness $h_s^{(m)}=\alpha_s\sqrt{t_m}$, where t_m is the maximum sedimentation duration under consideration. That is, the average value over the interval $0\le z\le h_s^{(m)}$, denoted by a line above the corresponding symbol, is equal to, for example, ρ_s:

$$\bar{\rho}_s=\frac{1}{h_s^{(m)}}\int_0^{h_s^{(m)}}\rho_s(z)dz, \tag{17}$$

and the averaged values of $\bar{\varphi}, \overline{\widetilde{\rho C}}_s, \bar{\lambda}_s, \bar{a}_s$ and other properties are defined analogously.

Within our model, the temperature (denote it $T_0^{(b)}$) at the base of the sedimentary sequence depends, among other parameters, on the coefficient α_s. According to expression (10), when z = 0 this temperature does not change with lithospheric age (and sediment-cover age) and equals

$$T_0^{(b)}=T_0(0,t)=T_1(0,t)=T_s+(T_{ph}-T_s)\frac{\mathrm{erf}(v)}{\mathrm{erf}(v)+\gamma\,\mathrm{erf}(u)}\ne \mathrm{f}(t). \tag{18}$$

As follows from Fig. 2, with increasing α_s, the temperature at the lithosphere surface, owing to the thermally insulating influence of accumulating sediments on the lithospheric thermal regime, can reach several hundreds of degrees Celsius. This indicates less efficient lithospheric cooling and, ultimately, slower growth of lithosphere thickness with time. At the same time, the dependence of $T_0^{(b)}(\alpha_s)$ on sediment material properties cannot be regarded as strong. The maximum relative discrepancy between values of $T_0^{(b)}(\alpha_s)$ within the plausible ranges of these parameters ($0.65\le\varphi_0\le 0.75$ and $0.4\le k_s\le 0.5$ km^{-1}) does not exceed ~16 %.

In our model, the indicator of the lithosphere cooling degree beneath sediments and the associated reduction in lithospheric thickness is the change in the value of the coefficient $\beta(\alpha_s)$ relative to its value $\beta(\alpha_s = 0)$ i. e., in the absence of sediments. Figure 2 clearly shows this decrease with increasing α_s, which is equivalent to a reduction in lithospheric thickness as sediment thickness $h_s(t)$ increases.

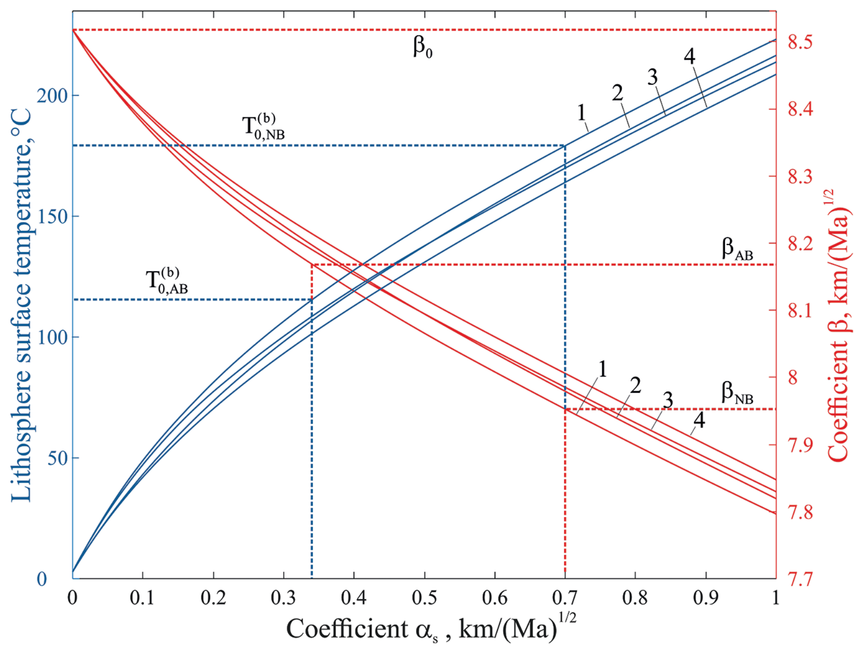

Fig. 2. Temperature $T_0^{(b)} = T_1(0,t)$ (in °C) at the lithosphere surface and the coefficient β as functions of the coefficient α_s. Graphs and scale in blue tones — $T_0^{(b)}(\alpha_s)$, in red — $\beta(\alpha_s)$. Sediments parameters: 1) $\varphi_0 = 0{,}75$, $k_s = 0{,}4$ km^{-1}; 2) $\varphi_0 = 0{,}65$, $k_s = 0{,}4$ km^{-1}; 3) $\varphi_0 = 0{,}75$, $k_s = 0{,}5$ km^{-1}; 4) $\varphi_0 = 0{,}65$, $k_s = 0{,}5$ km^{-1}

At $\alpha_s = 0$ this coefficient is equal to $\beta(0) \approx 8.52$ km/(Ma)$^{1/2}$. This value characterizes lithospheric thickness in the «open ocean» (without sediments). The dependence of $\beta(\alpha_s)$ on the sediment properties within the stated parameter ranges in the cover is less than 1 %.

2.2. Subsidence of the lithosphere with sediments and ocean depth

As the lithosphere ages, its thickness increases, and the weight of a vertical column of unit horizontal cross-section and height equal to that thickness also increases. As a consequence, the lithosphere subsides into the underlying asthenosphere, which is less dense and less viscous. If the lithosphere is overlain by a sedimentary layer, additional subsidence occurs under the weight of the sediments. The ocean depth Δh measured relative to the ridge crest, changes accordingly. Depending on sediment thickness (or equivalently the coefficient α_s) and sediment properties, the increment Δh may be either positive, meaning that the seafloor lies below the ridge crest, or negative, when sediment thickness is sufficiently large that the sediment surface lies above the ridge crest. We examine these isostatic conditions below.

At a distance from the spreading axis corresponding to lithospheric age t consider a thin vertical column whose upper boundary lies in the water column at the level of the ridge crest. The lower boundary of the column lies at the lithosphere–asthenosphere boundary, i. e. at depth $\Delta h(t) + h_s(t) + H_L(t)$ below the ridge crest. Comparing lithostatic pressure in this place with that at the same level beneath the ridge axis (in the viscous asthenosphere), we obtain $(\rho_w \Delta h + \bar{\rho}_s h_s + \bar{\rho}_L H_L) g = \rho_a g(\Delta h + h_s + H_L)$ (where g is gravitational acceleration), leading to the following expression for the increment $\Delta h(t)$ due to subsidence of the lithosphere together with the sediment layer, taking into account both its weight and its influence on lithospheric cooling:

$$\Delta h(t) = \frac{\bar{\rho}_L - \rho_a}{\rho_a - \rho_w} H_L(t) - \frac{\rho_a - \bar{\rho}_s}{\rho_a - \rho_w} h_s(t). \quad (19)$$

Here $\rho_a = \rho_L^0 (1 - \alpha_L T_m)$ is the density of asthenospheric material on the spreading axis, and ρ_w is the density of seawater. The average lithospheric density $\bar{\rho}_L$ is given by

$$\bar{\rho}_L(t) = -\frac{1}{\xi(t)} \int_{\xi(t)}^{0} \rho_L(z,t)\, dz, \quad (20)$$

where $\rho_L(z, t)$ is the density of lithospheric material at depth z, dependent on temperature at that point

$$\rho_L(z,t) = \rho_L^0\left[1 - \alpha_L T_1(z,t)\right], \tag{21}$$

here ρ_L^0 is the reference density of lithospheric and asthenospheric material, and α_L is the volumetric thermal expansion coefficient.

Substituting expression (21) into (20), we obtain

$$\bar{\rho}_L(t) = \rho_L^0\left[1 - \alpha_L \bar{T}_L(t)\right], \tag{22}$$

where $\bar{T}_L(t)$ is the average temperature of the lithosphere overlain by sediments. Taking into account expression (11) for $T_1(z, t)$, this mean average temperature does not vary with age:

$$\bar{T}_L(t) = -\frac{1}{\xi(t)}\int_{\xi(t)}^{0} T_1(z,t)dz = T_{ph} - \frac{\gamma\left(T_{ph} - T_s\right)\left[1 - \exp\left(-u^2\right)\right]}{\sqrt{\pi}u\left[\operatorname{erf}(v) + \gamma \operatorname{erf}(u)\right]} = \bar{T}_L \neq \mathrm{f}(t). \tag{23}$$

With equations (2), (9) and (22), expression (19) for ocean depth relative to the ridge crest takes the form

$$\Delta h(t) = \kappa\sqrt{t}, \tag{24}$$

where

$$\kappa = \kappa_L - \kappa_s, \qquad \kappa_L = \rho_L^0 \alpha_L \frac{T_m - \bar{T}_L}{\rho_a - \rho_w}\beta, \qquad \kappa_s = \frac{\rho_a - \bar{\rho}_s}{\rho_a - \rho_w}\alpha_s. \tag{25}$$

As follows from (24), (25), if $\kappa_s = \kappa_L$, complete compensation of lithospheric subsidence by sediments occurs. If $\kappa_s > \kappa_L$, then $\Delta h(t) < 0$ and the sediment surface lies above the ridge crest level.

The dependence κ on α_s is shown in Fig. 3a. The inset indicates, for each curve, the corresponding sediment parameters and the value α_s, at which complete compensation is achieved, i. e. $\kappa(\alpha_s) = 0$. Figure 3a demonstrates a noticeable sensitivity of the ocean depth $\Delta h(t)$ to the values of sediment parameters used in the calculations.

If the influence of the accumulating sedimentary cover on the thermal regime of the oceanic lithosphere is not taken into account, that is, if it is assumed that beneath the sediments the lithosphere is the same as in the open-ocean case, then, by constructing isostatic relations analogous to (19), we obtain the following expression for ocean depth $\Delta h_0(t)$ relative to the ridge crest:

$$\Delta h_0(t) = \kappa_0\sqrt{t}, \tag{26}$$

where

$$\kappa_0 = \kappa_L^0 - \kappa_s, \qquad \kappa_L^0 = \rho_L^0 \alpha_L \frac{T_m - \bar{T}_L^0}{\rho_a - \rho_w}\beta_0, \tag{27}$$

and κ_s, as before, is determined from equation (25), $\beta_0 = \beta(\alpha_s = 0)$, $\bar{T}_L^0 = \bar{T}_L(\alpha_s = 0)$.

The dependence $\kappa_0(\alpha_s)$ is shown in Fig. 3b. In the inset to this figure, for each curve, the corresponding values of sediment parameters and the values of α_s, at which complete compensation of lithospheric subsidence is achieved are also indicated. As follows from Fig. 3b, the coefficients $\kappa_0(\alpha_s)$ exceed the coefficients $\kappa(\alpha_s)$, in magnitude, indicating greater ocean depth in the case where the thermal influence of sediments on the lithosphere is neglected.

This difference becomes especially pronounced beginning at $\alpha_s > 0.3$, which implies significantly greater subsidence of the lithospheric surface and, consequently, of the seafloor, since sediment thickness is the same in both cases. It is also evident from this figure that the influence of sediment material properties (φ_0, k_s, ρ_{sk}) on the character of variation of $\kappa_0(\alpha_s)$ is qualitatively the same as their influence on $\kappa(\alpha_s)$.

3. On the evolution of sea depth in the Nansen and Amundsen Basins adjacent to the Gakkel Ridge

Using the results obtained above, we now estimate the causes of the substantially greater sea depths in the Amundsen Basin compared to those in the Nansen Basin. For this purpose, we consider the deep seismic section (Fig. 5) along profile MCS 2014-07 [6], which crosses both basins perpendicular to the spreading axis.

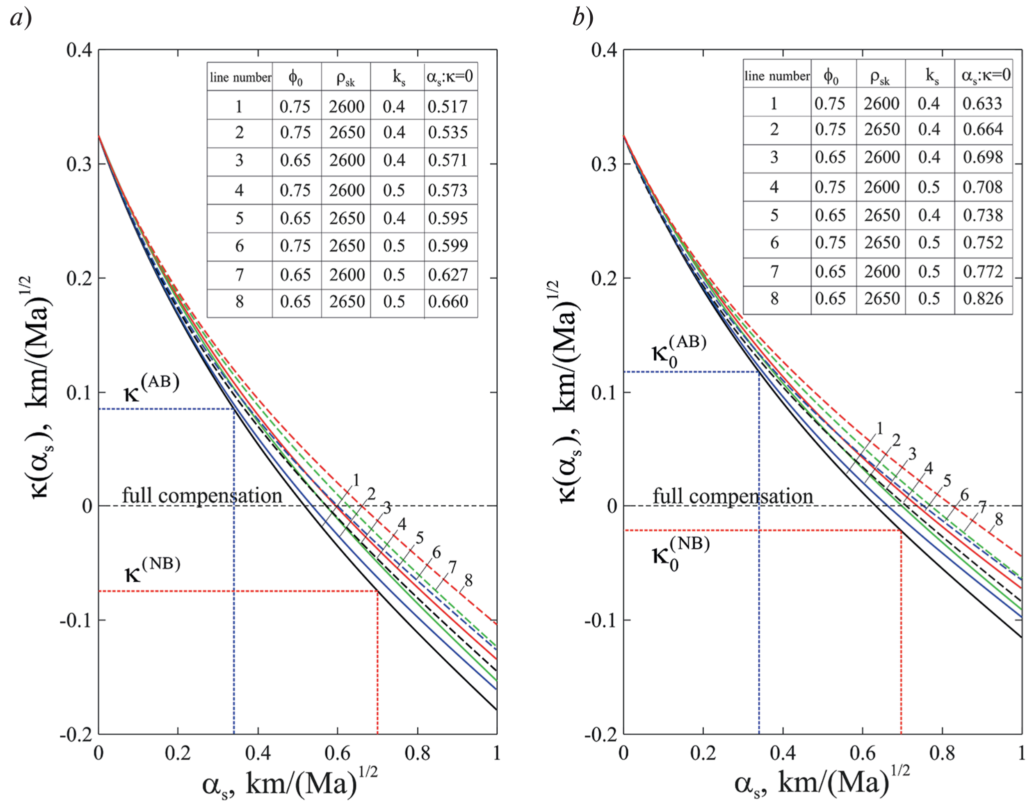

Fig. 3. Coefficient κ as a function of coefficient α_s: *a* — taking into account the influence of sedimentation on the formation of the oceanic lithosphere; *b* — ignoring this influence; α_s: κ = 0 — a value α_s such that κ = 0, i. e. with complete compensation for the subsidence of the lithosphere by sediments

In the oceanic lithosphere, including areas overlain by sediments, only extensional stresses generally operate (away from transform faults and subduction zones). Therefore, it is natural to expect that in the basins flanking the ultraslow-spreading Gakkel Ridge, the sedimentary layers would occur nearly horizontally. However, this configuration is not observed everywhere.

In the Nansen Basin, as follows from Fig. 5, up to approximately the 500 km mark along the profile, all seismic boundaries in the section, including the seafloor, rise significantly southward. This uplift occurs not only within the passive continental margin, but also above the oldest part of the oceanic lithosphere. This may be explained as follows. Immediately after continental lithosphere rupture, the newly formed oceanic lithosphere becomes attached to the continental lithosphere, then thickens as it cools while remaining continuously connected to it. Since the density of continental lithospheric rocks is substantially lower than that of oceanic lithosphere, the continental lithosphere possesses strong positive buoyancy in the asthenosphere. It therefore impedes the normal subsidence of the adjacent, oldest part of the oceanic lithosphere, whose buoyancy in the asthenosphere is negative and whose thickness increases with age. At the same time, under the load of the thickening oceanic lithosphere, the marginal part of the continental lithosphere undergoes additional subsidence relative to its position at the moment of rupture. This affects both sedimentation conditions and the inclination of sedimentary boundaries. With increasing distance from the continental margin, its influence on the subsidence behavior of the oceanic lithosphere should decrease.

North of the 500-kilometer mark on the profile, the lower seismic boundaries, as we see them, become subhorizontal. After the point ~520 km on this profile corresponding to the axis of linear magnetic anomaly with number 20 (lithosphere age is 44 million years), these boundaries are no longer traceable.

Taking the above into account, we select, along on the axis of linear magnetic anomaly 20 in the Nansen Basin, the point at a depth of $h_b \approx 8.1$ km, (outlined by a square in Fig. 5) as the base of the sedimentary cover.

The sea depth at this axis is $h_w \approx 3.4$ km, yielding a sediment thickness of approximately $h_s = h_b - h_w \approx$ ≈ 4.7 km. Since the age of the oceanic lithosphere at this location is $t = 44$ Ma, we obtain the value of the coefficient in the approximating relation (2) for sediment thickness as a function of lithospheric age $\alpha_s = \alpha_s^{(\text{HK})} \approx$ ≈ 0.7 km/(Ma)$^{1/2}$ in the approximating relation (2) for sediment thickness as a function of lithospheric age.

In the Amundsen Basin (AB), a similar pattern, although less pronounced than in the Nansen Basin, is observed north of 900 km mark_on the seismic section, when all reflecting boundaries, excluding the practically horizontal seafloor here, experience an uplift as they approach the Lomonosov Ridge whose lithosphere is continental one.)

At the profile point, corresponding to the position of the right linear anomaly axis with number 20, the sea depth is $h_w \approx 4.3$ km, and the base of the sedimentary cover is located at a depth $h_b \approx 6.6$ km. Thus, sediment thickness is approximately $h_s = h_b - h_w \approx 2.3$ km, which for the same lithospheric age $t = 44$ Ma corresponds to a specific value of the coefficient $\alpha_s = \alpha_s^{(\text{ÀÊ})} \approx 0.34$ km/(Ma)$^{1/2}$ in the approximating relation (2).

For sediment parameters in both basins, we adopt values typical of terrigenous basin infill: $\rho_{sk} = 2600$ kg/m^3, $\varphi_0 = 0.75$, $k_s = 0{,}4$ km^{-1}. The value of porosity φ_0 at the seafloor is substantiated and used in [1].

Using the obtained coefficients $\alpha_s^{(\text{HK})}$ and $\alpha_s^{(\text{AK})}$, we find, referring to Fig. 2 that the reduction of coefficient $\beta(\alpha_s)$ with increasing α_s from $\beta(0)$ (in the «open ocean») to $\beta(\alpha_s^{(\text{HK})})$ in the Nansen Basin amounts to $\Delta\beta = 0.75$ km/Ma$^{1/2}$. If the lithospheric age is taken as $t = 53$ Ma (the assumed time of opening of the central Eurasian Basin), then the lithosphere beneath sediments in the Nansen Basin will be thinner than lithosphere in the «open ocean» by $\Delta\beta\sqrt{t} \approx 4.15$ km. With $\beta(\alpha_s^{(\text{AK})})$ in the Amundsen Basin $\Delta\beta = 0.35$ km/Ma$^{1/2}$ and for the same age the corresponding reduction is smaller by $\Delta\beta\sqrt{t} \approx 2.55$ km compared to the «open ocean».

An estimate of the thermal influence of sedimentation on the lithosphere at $\alpha_s = \alpha_s^{(\text{HK})}$ and $t = 53$ Ma shows that in the Nansen Basin, sea depth is approximately 350–400 m smaller than in an ocean with the same sediment cover but without accounting for its thermal influence on the lithosphere (i. e., the difference between $\kappa(\alpha_s)$ and $\kappa_0(\alpha_s)$ in Fig. 3). In the Amundsen Basin at $\alpha_s = \alpha_s^{(\text{AK})}$ the analogous value is approximately 240 m.

The principal parameters of the oceanic lithosphere in both basins, calculated within the framework of the adopted dependence (2) of sediment thickness on lithospheric age, are presented in Table.

As follows from the table, within the adopted model, the average lithosphere temperature $\bar{T}_L = \bar{T}_L^{(\text{HK})}$ beneath the Nansen Basin exceeds $\bar{T}_L^{(\text{AK})}$ by 26K. At the same time, the temperature at the base of the sedimentary cover in the Nansen Basin is 64 K higher than in the Amundsen Basin. In contrast, the maximum lithosphere thickness $H_L^{(\max)}$ (at an age of 53 Ma) in the Amundsen Basin exceeds that of the lithosphere of the same age in the Nansen Basin by 16 km.

Table

Lithosphere parameters

Basin	β (km · Ma$^{-1/2}$)	$H_L^{(\max)}$ (km)	$\bar{T}_L$ (K/°C)	$T_0(0, t)$ (K/°C)	β_0 (km · Ma$^{-1/2}$)	$H_L^{(\max)}$ (km)	$\bar{T}_L$ (K/°C)
NB	7.95	57.9	959/685	463/179	8.52	62	887/614
AK	8.17	59.5	932/659	388/115	8.52	62	887/614

Because the density of oceanic lithospheric material substantially exceeds the average density of sediments, the lithosphere in the Amundsen Basin subsides to greater depths into the asthenosphere than in the Nansen Basin, despite the significantly greater thickness and average density of the sedimentary cover in the latter. As a result, the magnitude of lithospheric subsidence together with the overlying sediments differs between the two basins, equivalently, the increment of sea depth relative to the crest of the Gakkel Ridge is different in each case. This conclusion is clearly illustrated by the dependences of the calculated values $\zeta = \Delta h(t)$ and $\zeta = \Delta h_0(t)$, obtained using expressions (24) and (26), whose curves are shown in Fig. 4.

The calculated depths of both the seafloor and the base of the sedimentary cover have been superimposed on the same deep seismic section along profile MCS2014-07 (Fig. 5) [6]. As follows from this figure, our estimated sea depths in both the Nansen Basin and the Amundsen Basin, calculated taking into account not only the gravitational but also the thermal influence of sedimentation, are in quite satisfactory agreement with the observed values. Both the calculated (shown in orange) and the actual (shown in red) difference in sea depths at points in these basins with the same lithosphere age of 44 Ma differ only slightly.

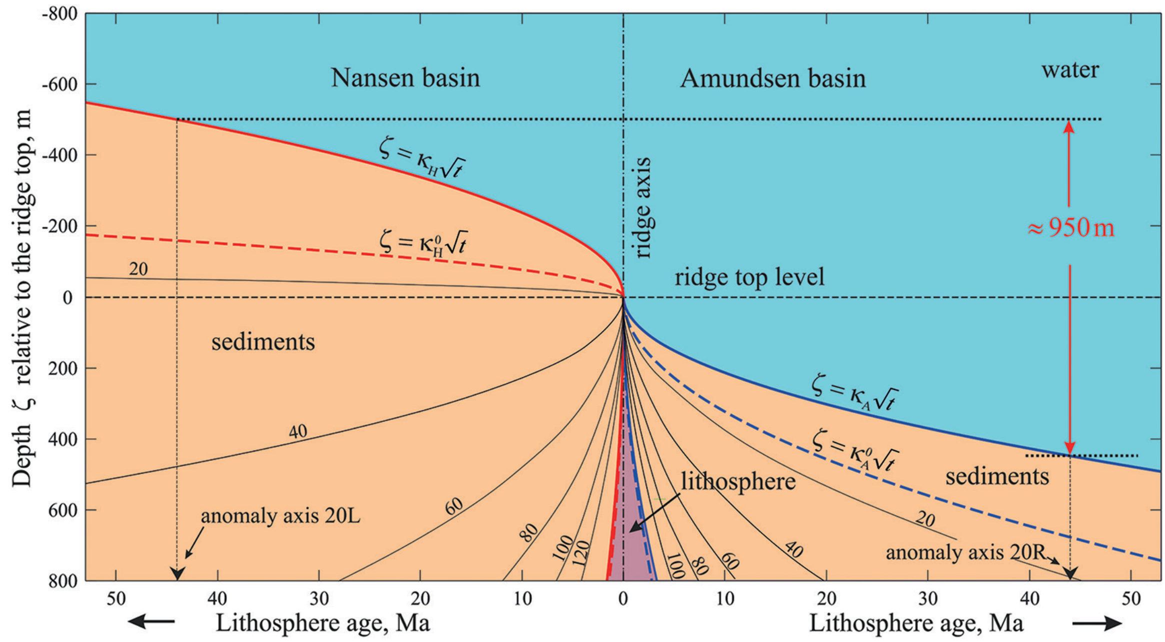

Fig. 4. Change in calculated ocean depth ζ(t) relative to the ridge crest. The red lines correspond to the Nansen Basin, and the blue lines to the Amundsen Basin. The dotted lines represent depths excluding the influence of sedimentation on the formation of the oceanic lithosphere, the thin lines with indices are temperature isolines and their values in °C

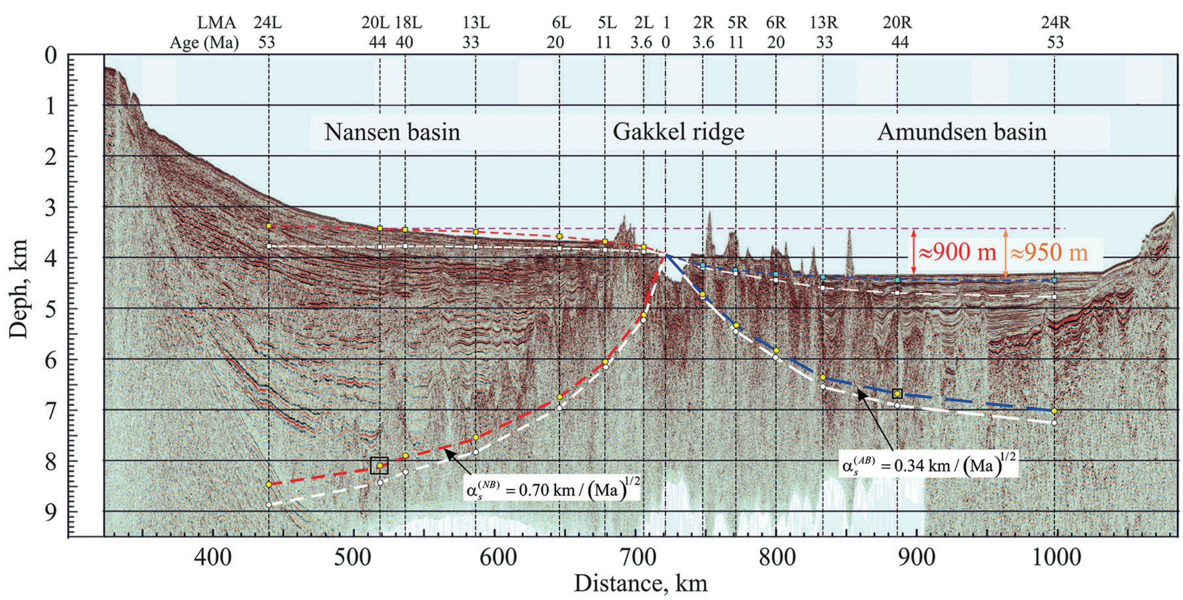

Fig. 5. Change in calculated and actual ocean depths relative to the ridge top. The red lines correspond to the Nansen Basin; the blue lines to the Amundsen Basin. The thin dotted line is the calculated sea depth relative to the Gakkel Ridge crest; the thick dotted line is the base of the sedimentary cover. The white dotted line represents the same surfaces, but without taking into account the thermal influence of sedimentation. LMA are linear magnetic anomalies, their numbers, and ages

4. Conclusions

Although the present study is of an evaluative character and is based on a single seismic profile using a simplified model of sedimentary cover formation in the basins, the results obtained allow the following conclusions to be drawn:

1. The sea depths in the Nansen and Amundsen basins, calculated for lithosphere of different ages taking into account both the gravitational and thermal effects of sedimentation, are in satisfactory agreement with the observed values. The calculated depth differences at reference points in the central parts of both basins are close to the actual.

2. The performed modeling of oceanic lithosphere formation, covered by accumulating sediments, in the Eurasian Basin of the Arctic Ocean, accounting for both gravitational and thermal influence of the sedimentation process, shows that the observed difference between depths of the Nansen and Amundsen basins is indeed controlled determined by the thicknesses of their sedimentary covers and is quite natural.

3. The use of only the gravitational influence of sedimentation, without accounting its the thermal influence, in isostatic schemes for determining sea depth may lead to errors of several hundred meters, since the sedimentation process itself changes the cooling regime of the oceanic lithosphere and therefore reduces its thickness.

4. The sedimentation process influences not only the thermal regime of the oceanic lithosphere but also the temperature distribution within the sedimentary cover itself. This must be taken into account when calculating indices of oceanic sediments maturity for hydrocarbon generation and when identifying oil and gas formation zones.

Funding

The research was carried out within the state assignment of Ministry of Science and Higher Education of the Russian Federation for IO RAS (theme No. FMWE-2024-0028).

Conflict of interests

The authors declare no conflict of interests.

References

1. Jokat W, Micksch U. Sedimentary structure of the Nansen and Amundsen basins, Arctic Ocean. Geophysical Research Letters. 2004;31: L02603. https://doi.org/10.1029/2003GL018352
2. Sorokhtin OG. Dependence of the mid-ocean ridges topography on the ocean floor spreading rate. *Report of the USSR Academy of Sciences*. 1973;208:1338–1341.
3. Athy LF. Density, porosity and compaction of sedimentary rocks. *AAPG Bulletin*. 1930;14:1–24.
4. Batsanin SF, Golmshtok AYa. On the thermal evolution of the oceanic lithosphere under sedimentation conditions. *Oceanology*. 1986;26(3):654–658.
5. Allen PA, Allen JR. Basin analysis. Oxford: Blackwell Scientific Publications; 1990. 451 p.
6. Kaminsky VD, editor. Arctic Basin (geology and morphology). St. Petersburg: VNIIOkeangeologia; 2017. 291 p. (In Russ.).

Литература

1. *Jokat W.*, *Micksch U.* Sedimentary structure of the Nansen and Amundsen basins, Arctic Ocean // Geophysical research letters. 2004. Vol. 31, L02603. https://doi.org/10.1029/2003GL018352
2. *Сорохтин О.Г.* Зависимость топографии срединно-океанических хребтов от скорости раздвижения дна океана // Доклады АН СССР. 1973. Т. 208. С. 1338–1341.

3. *Athy L.F.* Density, porosity and compaction of sedimentary rocks // AAPG Bul. 1930. No. 14. P. 1–24.
4. *Бацанин С.Ф.*, *Гольмшток А.Я.* О тепловой эволюции океанической литосферы в условиях осадконакопления // Океанология. 1986. Т. 26, № 3. С. 654–658.
5. *Allen P.A.*, *Allen J.R.* Basin analysis. Oxford: Blackwell Sci. Publ., 1990. 451 p.
6. Арктический бассейн (геология и морфология) / Ред. В.Д. Каминский. СПб.: ВНИИОкеангеология, 2017. 291 с.

About the authors

Alexander Ya. GOLMSHTOK, Cand.Sc. (Phys.-Math.), Chief Researcher, St. Petersburg Branch of IO RAS, Scopus AuthorID: 6602613595, SPIN-code (РИНЦ): 8068-9293, e-mail: golmshtok@gmail.com

Alexey L. PISKAREV, Dr. Sc. (Geol. and Mineral.), Chief Researcher, VNIIOkeangeologia; Prof. SPbU — Institute of Earth Sciences, ORCID: 0000-0002-6957-0242, e-mail: apiskarev@gmail.com